

3.23 Gamma-Ray Emission Cross Section From Proton-Incident Spallation Reaction

Kiminori IGA^{*1}, Kenji ISHIBASHI^{*1}, Nebuhiro SHIGYO^{*1}, Tatsushi NAKAMOTO^{*1},
 Keisuke MAEHATA^{*1}, Naruhiro MATSUFUJI^{*2}, Shin-ichirou MEIGO^{*3},
 Hiroshi TAKADA^{*3}, Satoshi CHIBA^{*3}, Masaharu NUMAJIRI^{*4},
 Takashi NAKAMURA^{*5}, Yukinobu WATANABE^{*6}

*1 Department of Nuclear Engineering, Kyushu University, Hakozaki, Higashi-ku, Fukuoka-shi 812-81.

*2 National Institute of Radiological Sciences, Anakawa, Inage-ku, Chiba-shi 263.

*3 Japan Atomic Energy Research Institute, Tokai-mura, Ibaraki-ken 319-11.

*4 National Laboratory for High Energy Physics, Oho, Tsukuba-shi, 305.

*5 Cyclotron Radioisotope Center, Tohoku University, Aramaki, Aoba-ku, Sendai-shi 980-77.

*6 Energy Conversion Engineering, Kyushu University, Kasuga-koen, Kasuga-shi 816.

e-mail: iga@kune2a.nucl.kyushu-u.ac.jp

Gamma-ray emission double differential cross sections from proton-incident spallation reaction have been measured at incident energies of 0.8, 1.5 and 3.0 GeV with Al, Fe, In and Pb targets. The experimental results have been compared with calculate values of HETC-KFA2. The measured cross sections disagree with the calculated results in the gamma ray energies above 10 MeV.

1. Introduction

Gamma-ray spectra from spallation reaction may show information about the target nucleus at excited state. However, the systematic experimental data have not been taken for the spallation reaction so far. Simulation codes such as HETC-KFA2⁽¹⁾ consider the gamma-ray emission with a simplified assumption, but their prediction adequacies have never been tested in detail for the spallation reaction. In this study we obtained the gamma-ray emission double differential cross sections by incident protons of a GeV range. The results were compared with HETC-KFA2.

2. Experiment

The experiment was carried out at the $\pi 2$ line of the 12 GeV proton synchrotron at National Laboratory for High Energy Physics. The experimental arrangement is illustrated in Fig. 1. Incident proton energies were 0.8, 1.5 and 3.0 GeV, and targets were Al, Fe, In and Pb. The detectors were placed in the directions of 15, 30, 60, 90, 120 and 150°. Since the primary purpose of this experiment was to measure neutrons by the TOF method, both gamma rays and neutrons were detected by $\Phi 5''$

$\times 5''$ and $\Phi 2'' \times 2''$ liquid scintillator NE213. The $\Phi 2'' \times 2''$ scintillator data, however, were not analyzed, because they produced unclear spectra for gamma rays of interest. The discrimination between gamma ray and neutron was accomplished by the two-gate integration method⁽²⁾. The example of ADC spectrum of gamma rays is shown in Fig. 2.

3. Analyses

The energies of ADC channels were corrected by gamma rays from checking sources of ^{137}Cs , ^{60}Co and Am-Be gamma rays up to 4.4 MeV. Above 4.4 MeV, we converted neutron energy that was measured by TOF method, into gamma-ray energy in terms of empirical expression by Cecil et al. ⁽³⁾

$$E_e = 0.83E_p - 2.82[1.0 - \exp(-0.25E_p^{0.93})] \quad (1)$$

where the electron energy E_e and the recoil proton energy E_p in detector are presented in units of MeV. The calibration result for ADC channel is plotted in Fig. 3.

The response functions of NE213 were calculated by EGS4 code⁽⁴⁾. The calculated response function for ^{60}Co gamma ray is presented in Fig. 4 together with measured one. Because of the poor energy resolution of NE213 the response function shows the sum of 1.173 MeV and 1.333 MeV gamma rays. The disagreement at lower energies was caused by background events. The response functions above 60 MeV are shown in Fig. 5. When incident gamma ray energies were higher than 60 MeV, the response functions of the scintillator are almost the same due to the use of small size NE213 containing low atomic number elements of C and H. This situation made it impossible to analyze gamma-ray spectra below 60 MeV.

Gamma-ray emission cross sections were obtained by unfolding ADC spectra by FERDo-U code⁽⁵⁾. The spectra contained a small amount of gamma rays that were created in scintillator by neutron: the peak at 4.4 MeV that made by $^{12}\text{C}(n,n')^{12}\text{C}^*$ reaction was eliminated by eye measure. Gamma-ray attenuation in targets was corrected by the simulation calculation with EGS4 code.

Experimental double differential cross sections are shown in Figs. 6, 7, 8 and 9 with the results of HETC-KFA2. The error bars indicate statistical ones and they are expressed only upper part for ease of looking. Since HETC-KFA2 calculates gamma-ray emission from the evaporation process, the results are isotropic and the same shape at different angles. The experimental results were in mostly good agreement with the results of HETC-KFA2 below 10 MeV, whereas the measured data are considerably larger than the calculation beyond this energy. Above 10 MeV, gamma rays may be emitted by such process as nuclear bremsstrahlung, preequilibrium processes, dipole resonance and high-spin state nucleus.

4. Conclusion

Gamma-ray emission double differential cross sections were obtained below 60 MeV. We compared the experimental results with the calculation results of HETC-KFA2. The experimental results are in good agreement with the calculation values only in the energy range of the evaporation process.

Acknowledgements

We gratefully acknowledge Prof. H. Hirayama and Dr. Y. Namito for use of EGS4, and Prof. S. Ban for use of FERDo-U.

References

- (1) Cloth, P., et al. : KFA-IRE-E AN/12/88 (1988)
- (2) Zucker, M. S., et al. : Nucl. Instrum. Methods, A299, 281 (1990)
- (3) Cecil, R. A., et al. : Nucl. Instrum. Methods, 161, 439 (1979)
- (4) Nelson, W. R., et al. : SLAC-Report-265 (1985)
- (5) Burrus, W. R. : ORNL-3743 (1965)

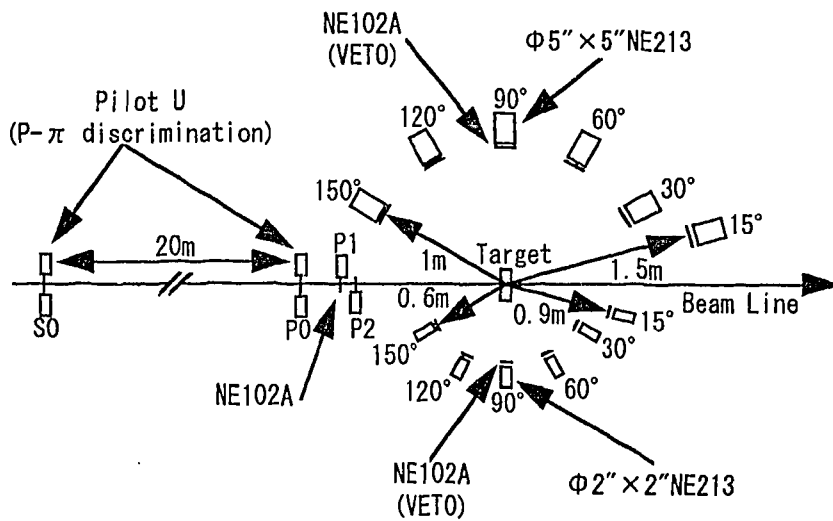


Fig.1 Illustration of experimental arrangement

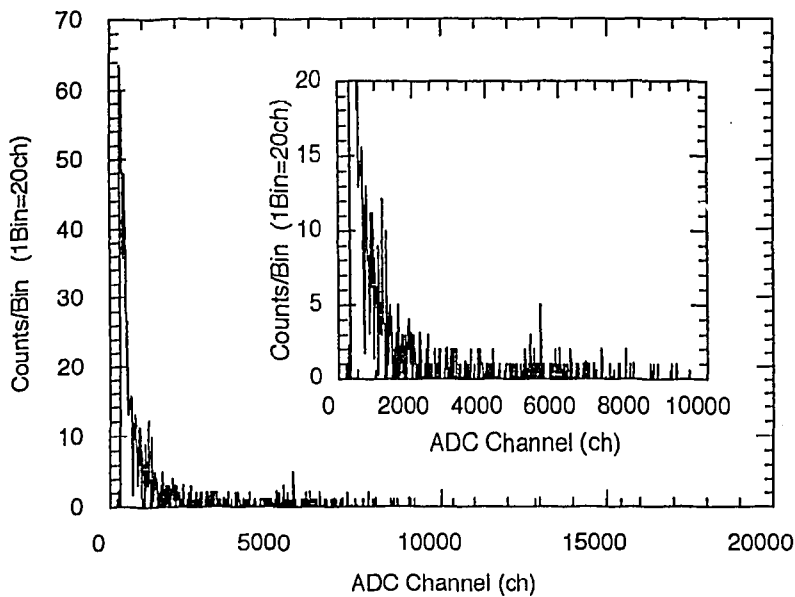


Fig. 2 ADC spectrum at 15deg by 0.8 GeV proton incident on Pb.

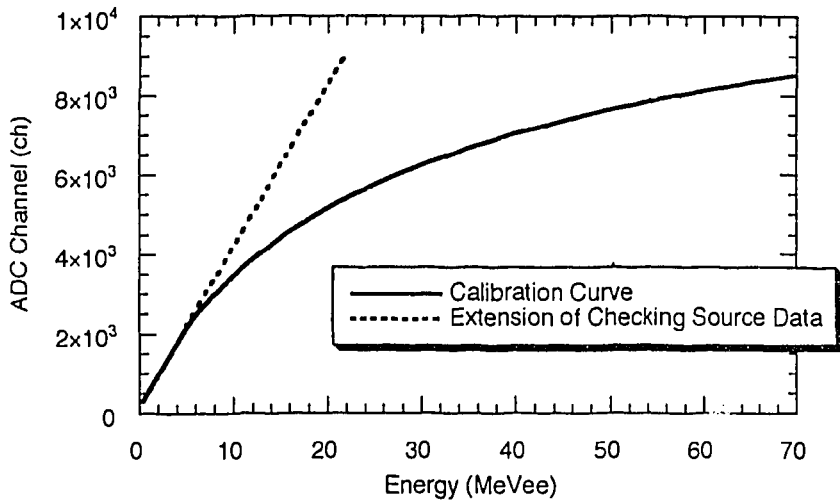


Fig. 3 Energy calibration for ADC channel for the detector.

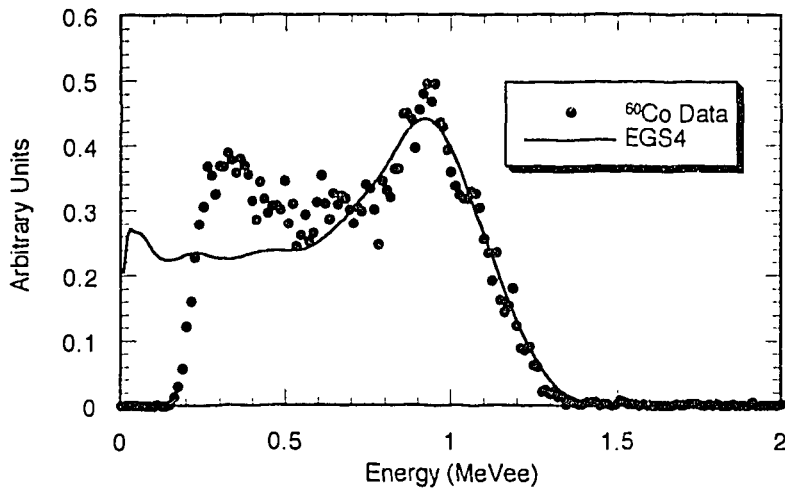


Fig. 4 Response functions from ^{60}Co gamma-ray source. The result as calculated was modified to take an actual energy resolution into consideration.

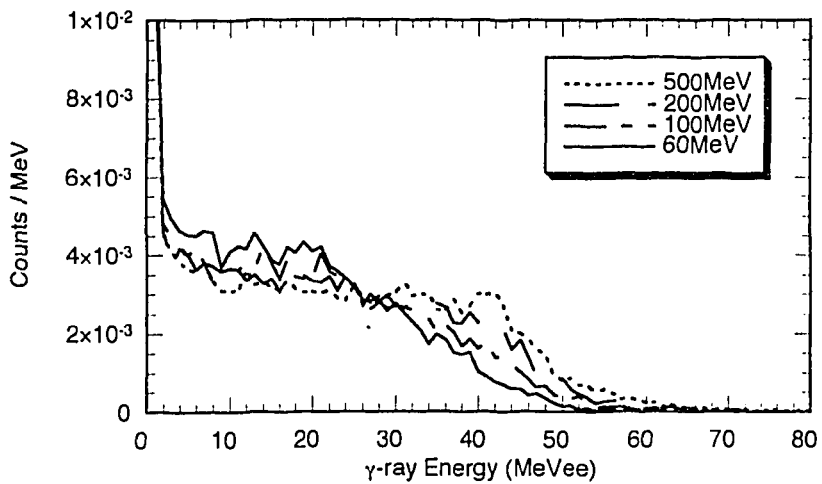


Fig. 5 Response functions for gamma rays with energies above 60 MeV.

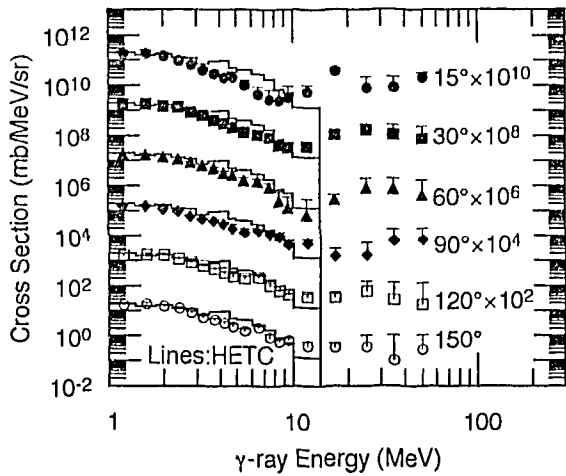


Fig. 6 (a) Gamma-ray spectra for 0.8GeV-proton incidence on Al.

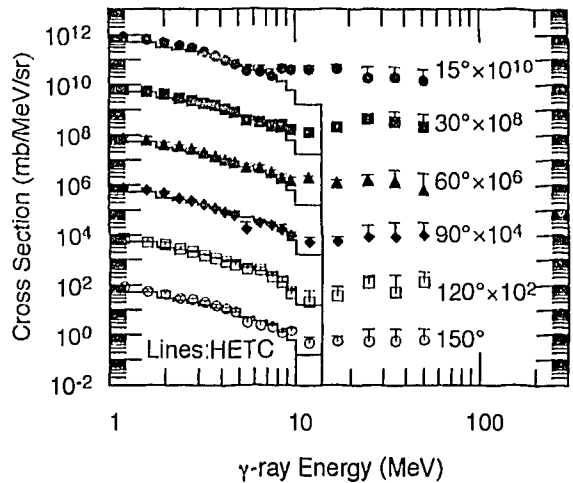


Fig. 7 (a) Gamma-ray spectra for 0.8GeV-proton incidence on Fe.

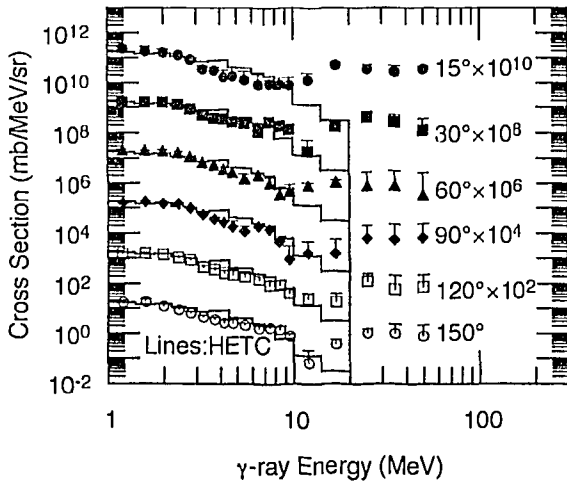


Fig. 6 (b) Gamma-ray spectra for 1.5GeV-proton incidence on Al.

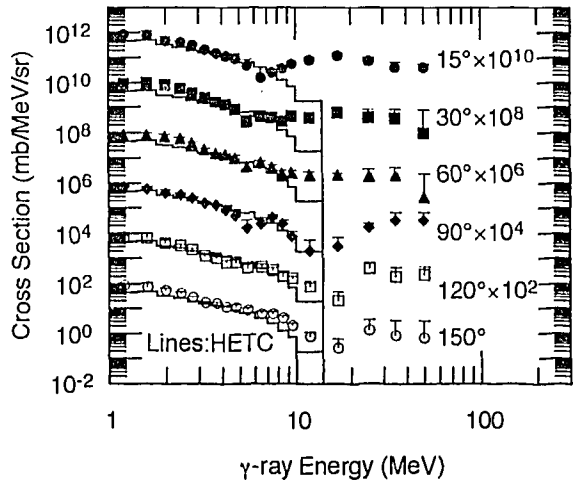


Fig. 7 (b) Gamma-ray spectra for 1.5GeV-proton incidence on Fe.

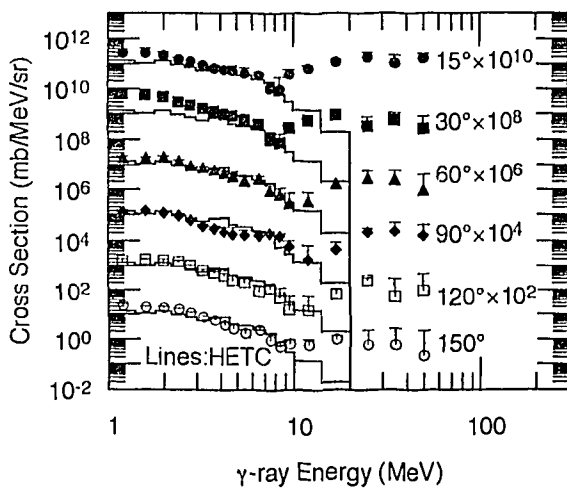


Fig. 6 (c) Gamma-ray spectra for 3.0GeV-proton incidence on Al.

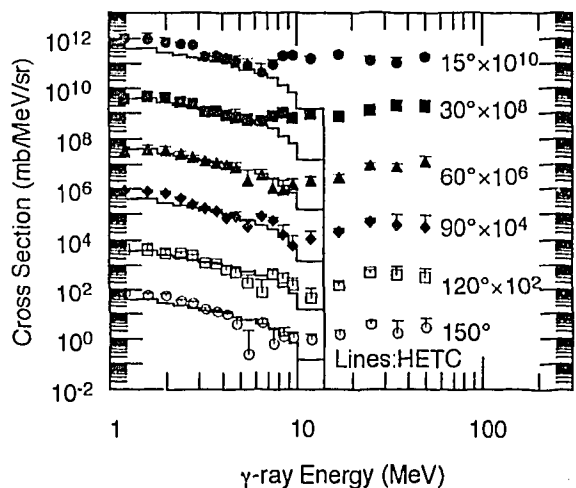


Fig. 7 (c) Gamma-ray spectra for 3.0GeV-proton incidence on Fe.

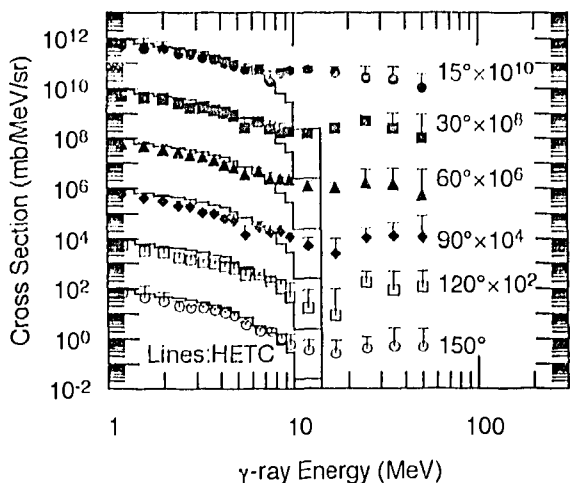


Fig. 8 (a) Gamma-ray spectra for 0.8GeV-proton incidence on In.

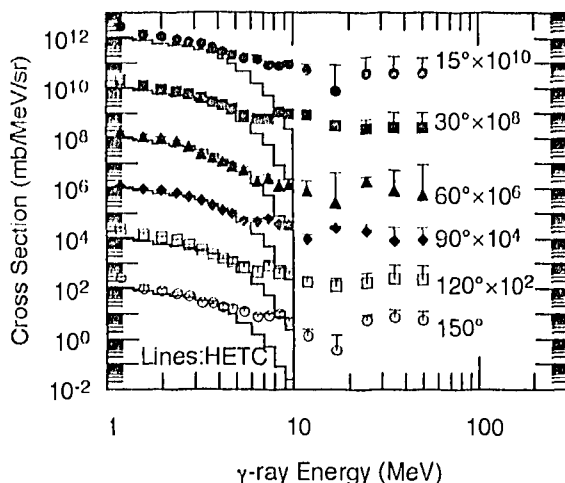


Fig. 9 (a) Gamma-ray spectra for 0.8GeV-proton incidence on Pb.

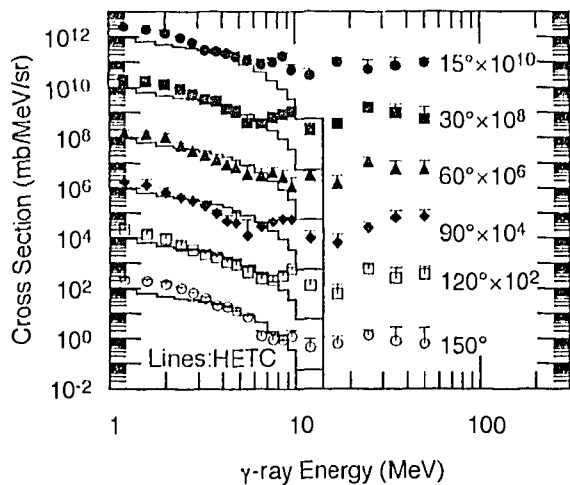


Fig. 8 (b) Gamma-ray spectra for 1.5GeV-proton incidence on In.

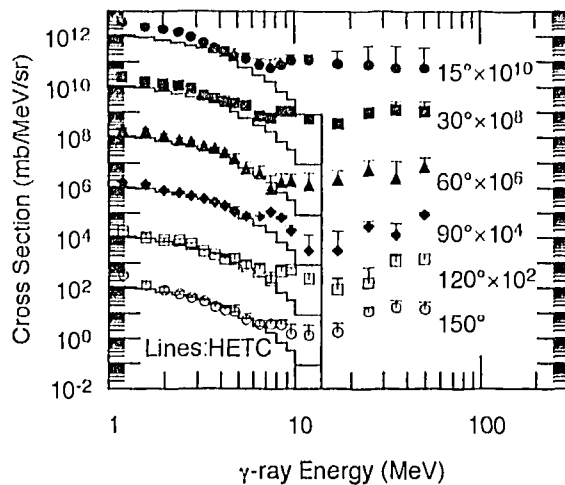


Fig. 9 (b) Gamma-ray spectra for 1.5GeV-proton incidence on Pb.

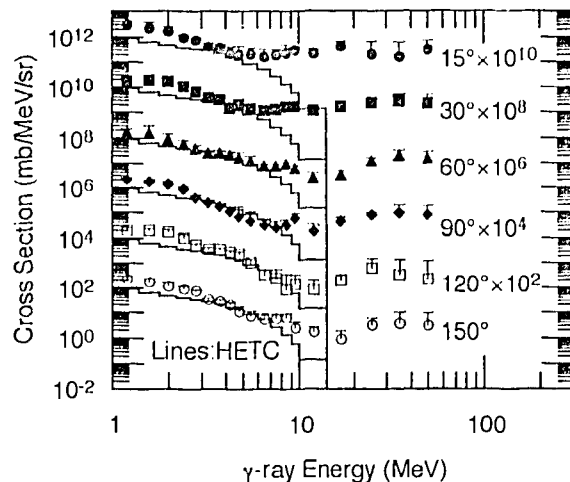


Fig. 8 (c) Gamma-ray spectra for 3.0GeV-proton incidence on In.

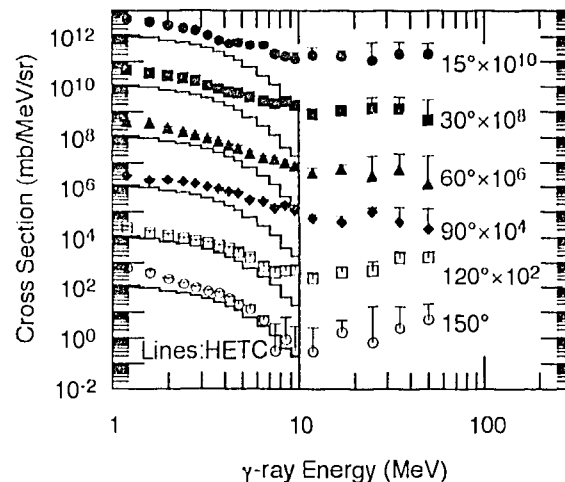


Fig. 9 (c) Gamma-ray spectra for 3.0GeV-proton incidence on Pb.